

Flux tubes in the $SU(3)$ vacuum: London penetration depth and coherence length

P. Cea L. Cosmai F. Cuteri* A. Papa

*Università della Calabria and INFN - Gruppo collegato di Cosenza

Lattice 2014 - The 32nd International Symposium on Lattice
Field Theory - June 25, 2014



Based on: Phys. Rev. D 89, 094505 - Published 19 May 2014

- 1 Introduction
 - Confinement and the dual superconductor model
 - Chromoelectric field on the lattice
- 2 Flux tubes on the lattice
 - Details about simulations
 - The measuring process at a glance
- 3 Numerical data
 - Results from the fit and parameters vs smearing
- 4 Penetration depth and coherence length
 - From lattice to physical units
 - Scaling
- 5 Conclusions



Outline

- 1 Introduction
 - Confinement and the dual superconductor model
 - Chromoelectric field on the lattice
- 2 Flux tubes on the lattice
 - Details about simulations
 - The measuring process at a glance
- 3 Numerical data
 - Results from the fit and parameters vs smearing
- 4 Penetration depth and coherence length
 - From lattice to physical units
 - Scaling
- 5 Conclusions



The color confinement problem

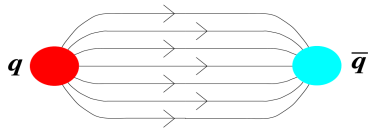


Figure: $q\bar{q}$ pair at distance R in the QCD vacuum

Deconfined phase

$$E_0(R) \xrightarrow{R \rightarrow \infty} 2m$$

Confined phase

$$E(R) \rightarrow \sigma R, \quad \sqrt{\sigma} = 420 \text{ MeV}$$

At the scale of color confinement non perturbative methods are needed



Dual superconductivity

Dual superconductor picture of confinement in QCD proposed by Mandelstam and 't Hooft.

[G. 't Hooft, in High Energy Physics, EPS International Conference, (1975)]

[S. Mandelstam, Phys. Rep. 23, (1976)]

QCD vacuum as a dual superconductor

- Color confinement due to the dual Meissner effect produced by the condensation of chromomagnetic monopoles
- Chromoelectric field connecting a $q\bar{q}$ static pair squeezed inside a tube structure: Abrikosov vortex

Relevance of nonperturbative study of chromoelectric flux tubes at $T \neq 0$ to clarify the formation of $c\bar{c}$ and $b\bar{b}$ bound states in heavy ion collisions.



Dual superconductivity

Dual superconductor picture of confinement in QCD proposed by Mandelstam and 't Hooft.

SUPERCONDUCTIVITY

$$F^{\mu\nu}$$

Electric charges condensate (Cooper pairs)

Magnetic Abrikosov flux tubes

DUAL SUPERCONDUCTIVITY

$$\tilde{F}^{\mu\nu}$$

Magnetic monopoles condensate

Chromoelectric dual Abrikosov flux tubes

Relevance of nonperturbative study of chromoelectric flux tubes at $T \neq 0$ to clarify the formation of $c\bar{c}$ and $b\bar{b}$ bound states in heavy ion collisions.



Dual superconductivity

Dual superconductor picture of confinement in QCD proposed by Mandelstam and 't Hooft.

SUPERCONDUCTIVITY

$$F_{\mu\nu}$$

Electric charges condensate (Cooper pairs)

Magnetic Abrikosov flux tubes

DUAL SUPERCONDUCTIVITY

$$\tilde{F}_{\mu\nu}$$

Magnetic monopoles condensate

Chromoelectric dual Abrikosov flux tubes

Relevance of nonperturbative study of chromoelectric flux tubes at $T \neq 0$ to clarify the formation of $c\bar{c}$ and $b\bar{b}$ bound states in heavy ion collisions.



Dual superconductivity

Dual superconductor picture of confinement in QCD proposed by Mandelstam and 't Hooft.

SUPERCONDUCTIVITY

$$F^{\mu\nu}$$

Electric charges condensate (Cooper pairs)

Magnetic Abrikosov flux tubes

DUAL SUPERCONDUCTIVITY

$$\tilde{F}^{\mu\nu}$$

Magnetic monopoles condensate

Chromoelectric dual Abrikosov flux tubes

Relevance of nonperturbative study of chromoelectric flux tubes at $T \neq 0$ to clarify the formation of $c\bar{c}$ and $b\bar{b}$ bound states in heavy ion collisions.



Dual superconductivity

Dual superconductor picture of confinement in QCD proposed by Mandelstam and 't Hooft.

SUPERCONDUCTIVITY

$$F_{\mu\nu}$$

Electric charges condensate (Cooper pairs)

Magnetic Abrikosov flux tubes

DUAL SUPERCONDUCTIVITY

$$\tilde{F}_{\mu\nu}$$

Magnetic monopoles condensate

Chromoelectric dual Abrikosov flux tubes

Relevance of nonperturbative study of chromoelectric flux tubes at $T \neq 0$ to clarify the formation of $c\bar{c}$ and $b\bar{b}$ bound states in heavy ion collisions.



Dual superconductivity

Dual superconductor picture of confinement in QCD proposed by Mandelstam and 't Hooft.

SUPERCONDUCTIVITY

$$F_{\mu\nu}$$

Electric charges condensate (Cooper pairs)

Magnetic Abrikosov flux tubes

DUAL SUPERCONDUCTIVITY

$$\tilde{F}_{\mu\nu}$$

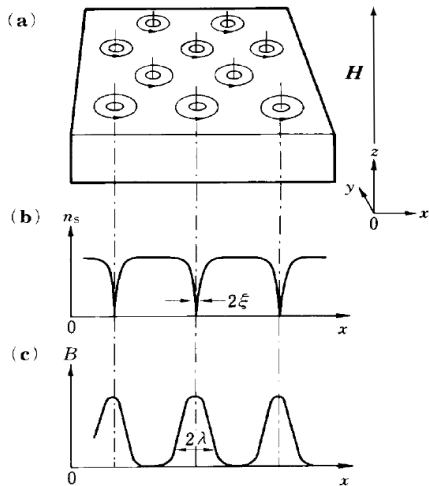
Magnetic monopoles condensate

Chromoelectric dual Abrikosov flux tubes

Relevance of nonperturbative study of chromoelectric flux tubes at $T \neq 0$ to clarify the formation of $c\bar{c}$ and $b\bar{b}$ bound states in heavy ion collisions.



Coherence length and London penetration depth



[A. C. Rose-Innes and E. H. Rhoderick, Introduction to Superconductivity (Pergamon Press, Second edition, 1978)]

- λ **London penetration depth**: characteristic length of the exponential decrease of \vec{B} in a superconductor
- ξ **Coherence length**: length scale on which the density of Cooper pairs can change appreciably



Fitting functions for $E_I(x_t)$ shape

Here enters the dual superconductor model

- Ordinary superconductivity: magnetic field as function of the distance from a vortex line in the mixed state
- Two different expressions coming, by dual analogy, from the London model or, equivalently, the Ginzburg-Landau theory

1 Vortex as a line singularity

$$E_I(x_t) = \frac{\phi}{2\pi} \mu^2 K_0(\mu x_t), \quad x_t > 0, \quad \lambda \gg \xi \leftrightarrow \kappa \gg 1$$

[P. Cea and L. Cosmai, Phys.Rev. D52 (1995)]

2 Cylindrical vortex

$$E_I(x_t) = \frac{\phi}{2\pi} \frac{1}{\lambda \xi_v} \frac{K_0(R/\lambda)}{K_1(\xi_v/\lambda)},$$

[J. R. Clem, J. Low Temp. Phys. 18, 427 (1975)]

[P. Cea, L. Cosmai, and A. Papa, Phys. Rev. D 86, (2012)]



Fitting function in our work

$$E_I(x_t) = \frac{\phi}{2\pi} \frac{\mu^2}{\alpha} \frac{K_0[(\mu^2 x_t^2 + \alpha^2)^{1/2}]}{K_1[\alpha]} \quad x_t \geq 0,$$

$$R = \sqrt{x_t^2 + \xi_v^2}, \quad \mu = \frac{1}{\lambda}, \quad \frac{1}{\alpha} = \frac{\lambda}{\xi_v}, \quad \kappa = \frac{\lambda}{\xi} = \frac{\sqrt{2}}{\alpha} [1 - K_0^2(\alpha)/K_1^2(\alpha)]^{1/2}.$$

- ① ϕ external flux
- ② $\mu = 1/\lambda$ London penetration depth inverse
- ③ $1/\alpha = \lambda/\xi_v$ with ξ_v variational core-radius parameter
- ④ $\kappa = \lambda/\xi$ Ginzburg-Landau parameter



Connected correlator from previous studies

$$\rho_W^{\text{conn}} = \frac{\langle \text{tr}(WLU_P L^\dagger) \rangle}{\langle \text{tr}(W) \rangle} - \frac{1}{N} \frac{\langle \text{tr}(U_P) \text{tr}(W) \rangle}{\langle \text{tr}(W) \rangle}$$

[A. Di Giacomo, M. Maggiore, S. Olejnik, Nucl.Phys. B347 (1990)]

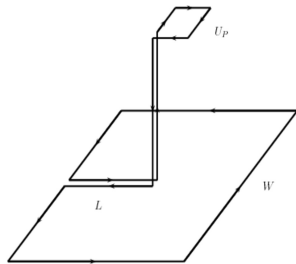
[P. Cea, L. Cosmai, Phys.Rev. D52 (1995)]

- Continuum limit

$$\rho_W^{\text{conn}} \xrightarrow{a \rightarrow 0} a^2 g \left[\langle F_{\mu\nu} \rangle_{q\bar{q}} - \langle F_{\mu\nu} \rangle_0 \right]$$

- Color field strength tensor

$$F_{\mu\nu}(x) = \sqrt{\frac{\beta}{2N}} \rho_W^{\text{conn}}(x)$$



- W Wilson loop
- L Schwinger line
- U_p Plaquette

- E_i(x), B_i(x) by changing U_P = U_{μν}(x) orientation.
- E_l(x_t) component dominates at T=0.



Connected correlator with Polyakov loops

$$\rho_P^{\text{conn}} = \frac{\langle \text{tr}(P(x) L U_P L^\dagger) \text{tr} P(y) \rangle}{\langle \text{tr}(P(x)) \text{tr}(P(y)) \rangle}$$

$$= \frac{1}{3} \frac{\langle \text{tr}(P(x)) \text{tr}(P(y)) \text{tr}(U_P) \rangle}{\langle \text{tr}(P(x)) \text{tr}(P(y)) \rangle}$$

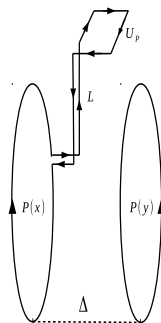
- Color field strength tensor

$$F_{\mu\nu}(x) = \sqrt{\frac{\beta}{6}} \rho_P^{\text{conn}}(x).$$

- ρ_P^{conn} suited for the $T \neq 0$ case

[A. Di Giacomo, M. Maggiore, S. Olejnik, Nucl.Phys. B347 (1990)]

[P. Skala, M. Faber, and M. Zach, Nucl. Phys. B494 (1997)]



- $P(x), P(y)$ Polyakov lines separated by a distance Δ
- L Schwinger line
- U_P Plaquette



Outline

- 1 Introduction
 - Confinement and the dual superconductor model
 - Chromoelectric field on the lattice
- 2 Flux tubes on the lattice
 - Details about simulations
 - The measuring process at a glance
- 3 Numerical data
 - Results from the fit and parameters vs smearing
- 4 Penetration depth and coherence length
 - From lattice to physical units
 - Scaling
- 5 Conclusions



Technicalities

Lattice and correlator features

- Size 20^4 and periodic boundary conditions
- Distance between Polyakov loops $\Delta = 4a, 6a, 8a$

LGT and action

- $SU(3)$ pure gauge LGT
- Wilson action $S = \beta \sum_{x, \mu > \nu} [1 - \frac{1}{3} \text{ReTr} U_{\mu\nu}(x)]$, with $5.9 < \beta < 6.1$

Algorithms

- Cabibbo-Marinari algorithm combined with overrelaxation
- APE smearing procedure to increase signal-to-noise ratio



Smearing procedure: motivations and method

- Replacement of the previously used cooling mechanism
- Possibility to check previous results in many different cases
 - ▶ Wilson correlator and Smearing
 - ▶ Polyakov correlator and Cooling
 - ▶ Polyakov correlator and Smearing

APE smearing procedure

[Albanese et al., Phys. Lett. B 192 (1987)] [Bonnet et al., Phys. Rev. D 62 (2000)]

$$C_{\mu\nu}(x) = U_\nu(x)U_\mu(x + \hat{\nu})U_\nu^\dagger(x + \hat{\mu}) \\ + U_\nu^\dagger(x - \hat{\nu})U_\mu(x - \hat{\nu})U_\nu(x - \hat{\nu} + \hat{\mu})$$

$$\tilde{U}_\mu(x) = \mathcal{P}_{SU(3)}[(1 - \alpha)U_\mu(x) + \frac{\alpha}{6} \sum_{\mu \neq \nu} C_{\mu\nu}(x)],$$

$$\alpha = 0.5,$$

$$16 < n_{ape} < 50$$



Our investigation in few steps

For different values of β

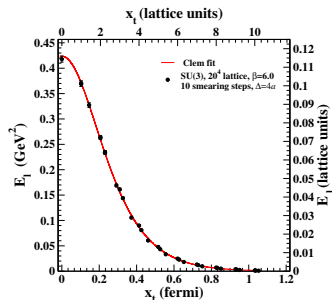
- Smearing over a thermalized field configuration
- Measurement of $E_I(x_t)$ through ρ_P^{conn} by varying plaquette position
- Fit of the shape of $E_I(x_t)$ to extract the parameters $\phi, \mu, \lambda/\xi_v, \kappa$
- Analysis of the behavior of $\phi, \mu, \lambda/\xi_v, \kappa$ with smearing, looking for a plateau
- Estimate of λ and ξ from a scaling analysis



Our investigation in few steps

For different values of β

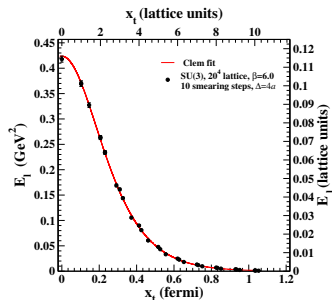
- Smearing over a thermalized field configuration
- Measurement of $E_I(x_t)$ through ρ_P^{conn} by varying plaquette position
- Fit of the shape of $E_I(x_t)$ to extract the parameters ϕ , μ , λ/ξ_v , κ
- Analysis of the behavior of ϕ , μ , λ/ξ_v , κ with smearing, looking for a plateau
- Estimate of λ and ξ from a scaling analysis



Our investigation in few steps

For different values of β

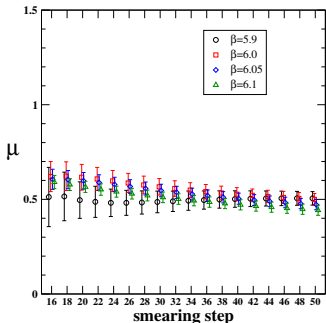
- Smearing over a thermalized field configuration
- Measurement of $E_l(x_t)$ through ρ_P^{conn} by varying plaquette position
- Fit of the shape of $E_l(x_t)$ to extract the parameters ϕ , μ , λ/ξ_v , κ
- Analysis of the behavior of ϕ , μ , λ/ξ_v , κ with smearing, looking for a plateau
- Estimate of λ and ξ from a scaling analysis



Our investigation in few steps

For different values of β

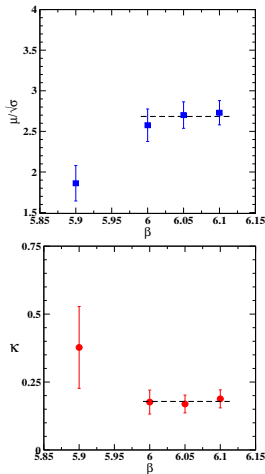
- Smearing over a thermalized field configuration
- Measurement of $E_l(x_t)$ through ρ_P^{conn} by varying plaquette position
- Fit of the shape of $E_l(x_t)$ to extract the parameters ϕ , μ , λ/ξ_v , κ
- Analysis of the behavior of ϕ , μ , λ/ξ_v , κ with smearing, looking for a plateau
- Estimate of λ and ξ from a scaling analysis



Our investigation in few steps

For different values of β

- Smearing over a thermalized field configuration
- Measurement of $E_l(x_t)$ through ρ_P^{conn} by varying plaquette position
- Fit of the shape of $E_l(x_t)$ to extract the parameters ϕ , μ , λ/ξ_v , κ
- Analysis of the behavior of ϕ , μ , λ/ξ_v , κ with smearing, looking for a plateau
- Estimate of λ and ξ from a scaling analysis



Outline

- 1 Introduction
 - Confinement and the dual superconductor model
 - Chromoelectric field on the lattice
- 2 Flux tubes on the lattice
 - Details about simulations
 - The measuring process at a glance
- 3 Numerical data**
 - Results from the fit and parameters vs smearing
- 4 Penetration depth and coherence length
 - From lattice to physical units
 - Scaling
- 5 Conclusions



Results from the fit and parameters vs smearing

Measurements at integer and noninteger distances

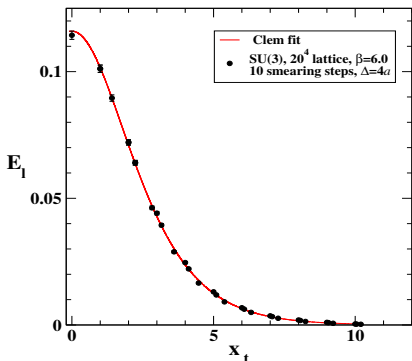


Figure: Longitudinal chromoelectric field E_l versus x_t , in lattice units for $\Delta = 4a$ and after 10 smearing steps

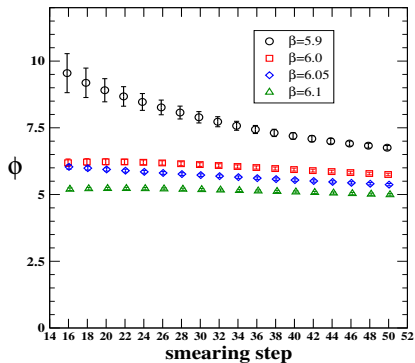
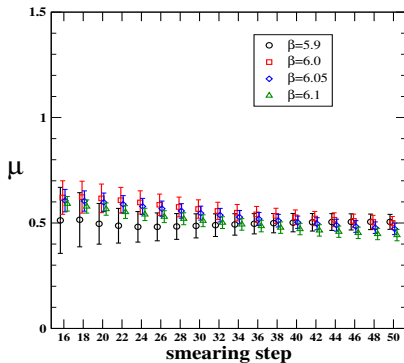
- Noninteger distances included to check for rotational invariance restoration
- Restriction only to points at integer distances:
 - ▶ Smaller χ_r^2
 - ▶ CPU time saved

Consistent values for parameters in both cases



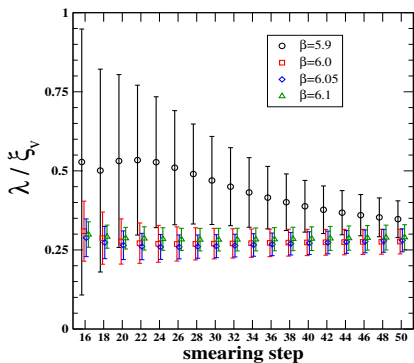
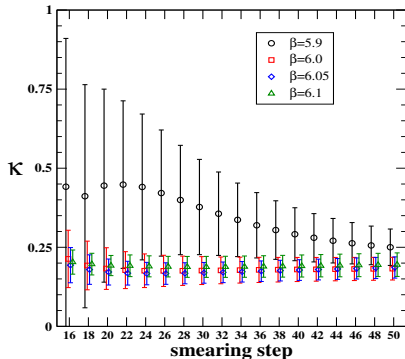
Results from the fit and parameters vs smearing

Parameters vs smearing: looking for a plateau

Figure: ϕ vs smearing ($\Delta = 6a$)Figure: μ vs smearing ($\Delta = 6a$)

Results from the fit and parameters vs smearing

Parameters vs smearing: looking for a plateau

Figure: λ / ξ_v vs smearing ($\Delta = 6a$)Figure: κ vs smearing ($\Delta = 6a$)

Results from the fit and parameters vs smearing

Plateau values vs β comparing all the sizes

Δ variation to study contamination effects due to the proximity of the static color sources.

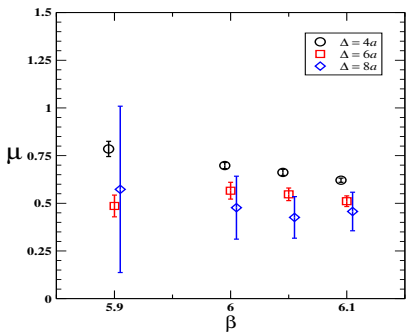


Figure: Plateau values for μ vs β
($\Delta = 4a, 6a, 8a$)

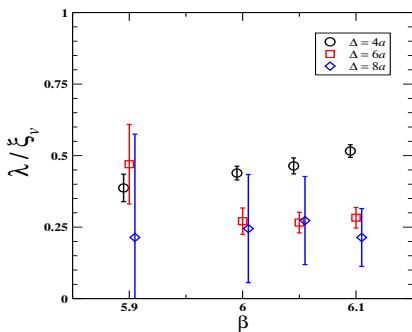


Figure: Plateau values for λ/ξ_v vs β
($\Delta = 4a, 6a, 8a$)

$\Delta = 6a$ good compromise between contaminations and signal-to-noise.



Outline

- 1 Introduction
 - Confinement and the dual superconductor model
 - Chromoelectric field on the lattice
- 2 Flux tubes on the lattice
 - Details about simulations
 - The measuring process at a glance
- 3 Numerical data
 - Results from the fit and parameters vs smearing
- 4 Penetration depth and coherence length
 - From lattice to physical units
 - Scaling
- 5 Conclusions



Setting the scale

Scaling of the plateau values of $a\mu$ with the string tension through the parametrization.

$$\begin{aligned}\sqrt{\sigma}(g) &= f_{\text{SU}(3)}(g^2)[1 + 0.2731 \hat{a}^2(g) \\ &\quad - 0.01545 \hat{a}^4(g) + 0.01975 \hat{a}^6(g)]/0.01364\end{aligned}$$

$$\hat{a}(g) = \frac{f_{\text{SU}(3)}(g^2)}{f_{\text{SU}(3)}(g^2(\beta = 6))}, \quad \beta = \frac{6}{g^2}, \quad 5.6 \leq \beta \leq 6.5$$

$$f_{\text{SU}(3)}(g^2) = (b_0 g^2)^{\frac{-b_1}{2b_0^2}} \exp\left(\frac{-1}{2b_0 g^2}\right), \quad b_0 = \frac{11}{(4\pi)^2}, \quad b_1 = \frac{102}{(4\pi)^4}$$

[R. G. Edwards, U. M. Heller, and T. R. Klassen, Nucl. Phys. B 517, (1998)]



Field in lattice and physical units

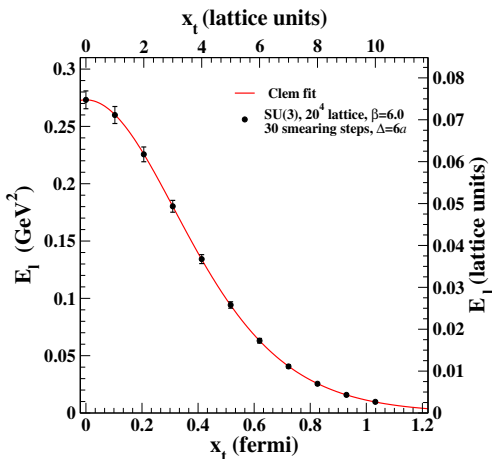
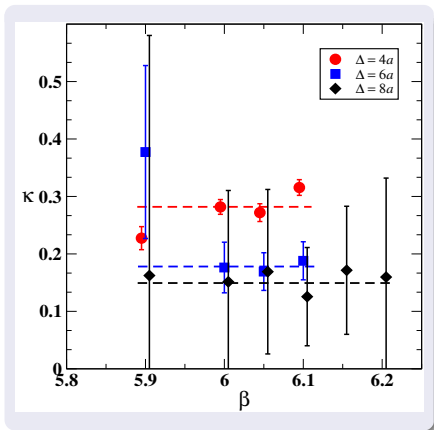
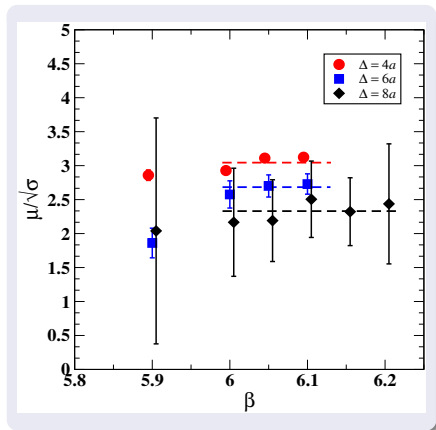


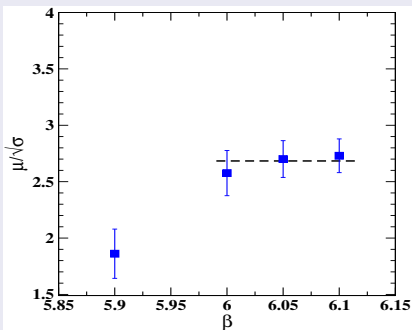
Figure: Longitudinal chromoelectric field E_l versus x_t , in lattice units and in physical units, for $\Delta = 6a$ and after 30 smearing steps



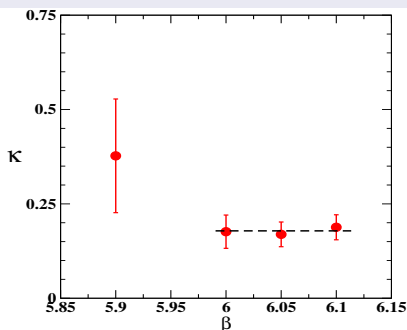
Parameters scaling behavior: sizes compared



Scaling

Parameters scaling behavior: $\Delta = 6a$ 

$$\mu/\sqrt{\sigma} = 2.684(97) \quad \mu/\sqrt{\sigma}_{old} = 2.799(38)$$



$$\kappa = 0.178(21) \quad \kappa_{old} = 0.243(88)$$

$$\lambda = 1/\mu = 0.1750(63) \text{ fm}$$

$$\xi = 0.983(121) \text{ fm}$$

Here 'old' means Wilson connected correlator and cooling as in
 [P. Cea, L. Cosmai, and A. Papa, Phys. Rev. D 86, (2012)]



Outline

- 1 Introduction
 - Confinement and the dual superconductor model
 - Chromoelectric field on the lattice
- 2 Flux tubes on the lattice
 - Details about simulations
 - The measuring process at a glance
- 3 Numerical data
 - Results from the fit and parameters vs smearing
- 4 Penetration depth and coherence length
 - From lattice to physical units
 - Scaling
- 5 Conclusions



Summary and outlook

- SU(3) vacuum as a type-I dual superconductor in agreement with [A. Shibata, K.-I. Kondo, S. Kato, and T. Shinohara, Phys. Rev. D 87, (2013)]
 - λ in agreement with [P. Cea, L. Cosmai, and A. Papa, Phys. Rev. D 86, (2012)][P. Bicudo, M. Cardoso, and N. Cardoso, PoS LATTICE2013 (2014) 495]
 - Relation to the “intrinsic width” of the flux tube [M. Caselle and P. Grinza, J. High Energy Phys. 11 (2012) 174.] to be investigated
-
- Finite temperature
 - Introduction of dynamical quarks d.o.f. (implementation of ρ_P^{conn} within the MILC code)
 - Check of the validity of the model (goodness of the fit): R and x_t ranges



THANK YOU